

Possible spin-triplet superconductivity in $\text{Na}_x\text{CoO}_2 \cdot y\text{H}_2\text{O}$ – ^{59}Co NMR study –

M. Kato^{†‡}, C. Michioka[†], T. Waki[†], Y. Itoh[†], K. Yoshimura[†],
 K. Ishida[§], H. Sakurai^{||}, E. Takayama-Muromachi^{||}, K.
 Takada[¶] and T. Sasaki[¶]

[†] Department of Chemistry, Graduate School of Science, Kyoto University, Kyoto
 606-8502, Japan

[§] Department of Physics, Graduate School of Science, Kyoto University, Kyoto
 606-8502, Japan

^{||} Superconducting Materials Center, National Institute for Materials Science, 1-1
 Namiki, Tsukuba, Ibaraki 305-0044, Japan

[¶] Advanced Materials Laboratory, National Institute for Materials Science, Namiki
 1-1, Tsukuba, Ibaraki 305-0044, Japan

E-mail: makato@mail.doshisha.ac.jp

Abstract. We report ^{59}Co NMR studies on the magnetically oriented powder samples of Co-oxide superconductors $\text{Na}_x\text{CoO}_2 \cdot y\text{H}_2\text{O}$ with $T_c \sim 4.7\text{K}$. From two-dimensional powder pattern in the NMR spectrum, the ab -plane Knight shift in the normal state was estimated by the magnetic field dependence of second-order quadrupole shifts at various temperatures. Below 50 K, the Knight shift shows a Curie-Weiss-like temperature dependence, similarly to the bulk magnetic susceptibility χ . From the analysis of so-called K - χ plot, the spin and the orbital components of K and the positive hyperfine coupling constant were estimated. The onset temperature of superconducting transition in the Knight shift does not change so much in an applied magnetic field up to 7 T, which is consistent with the reported high upper critical field H_{c2} . The Knight shift at 7 T shows an invariant behavior below T_c . No coherence peak just below T_c was observed in the temperature dependence of the nuclear spin-lattice relaxation rate $1/T_1$ in both cases of NMR and NQR. We conclude that the invariant behavior of the Knight shift below T_c and unconventional behaviors of $1/T_1$ possibly indicate the spin-triplet superconductivity with p - or f -wave symmetry.

Submitted to: *J. Phys.: Condens. Matter*

PACS numbers: 74.70-b, 76.60-k, 74.20.Rp

[‡] Present address: Department of Molecular Science and Technology, Faculty of Engineering, Doshisha University, Kyotanabe, Kyoto 610-0394, Japan.

1. Introduction

Recent discovery of superconductivity in $\text{Na}_x\text{CoO}_2 \cdot y\text{H}_2\text{O}$ with the transition temperature (T_c) of about 4.7 K [1] has been a major breakthrough in search for novel layered transition metal oxide superconductors. $\text{Na}_x\text{CoO}_2 \cdot y\text{H}_2\text{O}$ has a two-dimensional (2D) crystal structure where Co atoms form a 2D triangular lattice separated by Na^+ ions and H_2O molecules. The intercalation of H_2O molecules leads to an increase of the c -axis lattice constant, which is considered to enhance two dimensionality of CoO_2 layers. The triangular configuration on the CoO_2 plane potentially has a possibility of an unconventional superconductivity by marvelous mechanism in the novel quantum state, as suggested by many theoretical works. For example, Tanaka *et al.* indicated that the spin-triplet superconductivity may be realized with similar pairing process to Sr_2RuO_4 since the hexagonal structure in $\text{Na}_x\text{CoO}_2 \cdot y\text{H}_2\text{O}$ is favorite for a spin-triplet pairing [2]. Some groups studied a single band t - J model as a prototype of strong coupling electrons theories to understand the low energy electronic phenomena based on the resonating-valence-bond (RVB) state [3, 4, 5, 6, 7]. Kuroki *et al.* introduced a single band effective model with taking into account pocket-like Fermi surfaces along with van Hove singularity near the K point in the first Brillouin zone [8, 9, 10, 11]. They showed that the large density of states near the Fermi level gives rise to ferromagnetic spin fluctuations, leading to the f -wave superconductivity due to disconnected Fermi surfaces near the Γ point. Khaliullin *et al.* emphasized the importance of a spin-orbit (LS) coupling, and showed that the hole carriers with pseudo-spin one-half on a f level, separated from t_{2g} -orbital degeneracy due to trigonal distribution and spin-orbit interaction, makes the spin-triplet state always be favored [12].

In order to clarify the superconducting mechanism in $\text{Na}_x\text{CoO}_2 \cdot y\text{H}_2\text{O}$, it is very important to investigate the Cooper-pair symmetry. Nuclear magnetic resonance (NMR) is known as a powerful probe to investigate the pairing symmetry in the superconducting state. In this paper, we report the detailed experimental results of Knight shift, K , and the spin-lattice relaxation rate, $1/T_1$, in $\text{Na}_x\text{CoO}_2 \cdot y\text{H}_2\text{O}$ obtained by ^{59}Co NMR and nuclear quadrupole resonance (NQR) measurements. We demonstrate that K_y , one of the in-plane Knight shifts is invariant below T_c at a high field of about 7 T, where $1/T_1$ drops at T_c and obeys T^3 law without the coherence peak just below T_c . These results are attributable to the possible formation of p - or f -wave superconducting state with line-nodes on the superconducting gap. Our results are inconsistent with the previous report by Kobayashi *et al.*, which suggested spin-singlet s -wave superconductivity from the result of a lower field of about 2 T [13]. However, the precise values of the Knight shift cannot be estimated without explaining the frequency dependence of field-swept spectra because of the coexistence of electric quadrupole and Zeeman interactions. Thus, we clearly present how to estimate the spin part of the Knight shift using the frequency dependence of resonance fields above T_c . The full analysis of the NMR parameters is crucially important for discussing the Cooper-pair symmetry in the superconducting state.

2. Experiments

The powder sample of $\text{Na}_x\text{CoO}_2 \cdot y\text{H}_2\text{O}$ was prepared by the oxidation process from the mother compound, $\text{Na}_{0.7}\text{CoO}_2$ [1]. The obtained sample was confirmed to be a single phase by the powder X-ray diffraction (XRD) measurement. The chemical compositions of Na and H_2O were found to be about 0.35 and 1.3, respectively, by inductively coupled plasma atomic emission spectroscopy (ICP) [1]. The superconducting transition temperature (T_c) was estimated from the temperature dependence of the magnetization using SQUID magnetometer. ^{59}Co NMR and NQR measurements were performed by the spin-echo method with a standard phase coherent-type pulsed spectrometer. The powder sample was oriented and fixed by using an organic solvent hexane under the condition of the external field, $H = 8$ T. In our NMR measurement, hexane was found to be an optimal agent to fix the sample because it has the melting point of 178 K and does not absorb water molecules. Stycast 1266, which is useful for high T_c cuprates superconductors, were not suitable owing to their desiccating effect. From the XRD measurement, we found that the c -axis of the sample was oriented perpendicular to the external magnetic field H and that the random orientation in the c -plane was obtained along H . Since the orientation and the NMR measurements were performed at the same time, the magnetic field in NMR was applied completely to the same direction where the sample was aligned. NQR measurements were performed in zero field. $1/T_1$ was estimated by monitoring the recovery of the spin-echo amplitude, $M(t)$, after an inversion pulse as a function of the delayed time (t) between an inversion π and the observation radio-frequency $\pi/2 - \pi$ pulses.

Once the sample was cooled, it was kept below 100 K even during the intermission of NMR and NQR measurements. We must maintain a degree of the orientation throughout the measurements because the resonance fields for peaks and shoulders of the NMR spectrum are sensitive to the sample orientation. We also notice that it is extremely important to avoid the deficiency of H_2O molecules since the superconducting properties such as T_c are sensitive to the H_2O content [14].

3. Results and discussion

3.1. ^{59}Co Knight shift above T_c

Figure 1 shows a typical ^{59}Co NMR spectrum of $\text{Na}_x\text{CoO}_2 \cdot y\text{H}_2\text{O}$ at a frequency of 59.200 MHz. The observed NMR spectrum can be understood by a 2D powder pattern with anisotropic Knight shifts and the second order quadrupole interaction. We have succeeded in determining these NMR parameters from the following analysis.

In order to determine the Knight shift above T_c , we use the central transition line ($+1/2 \leftrightarrow -1/2$) as shown in Fig. 2. We assume that principal axes of the Knight shift tensor coincide with those of the electric-field gradient (EFG) tensor. This assumption is generally rational because those tensors are mainly governed by the local symmetry around the Co site. Because of the quadrupole effect up to the second-order

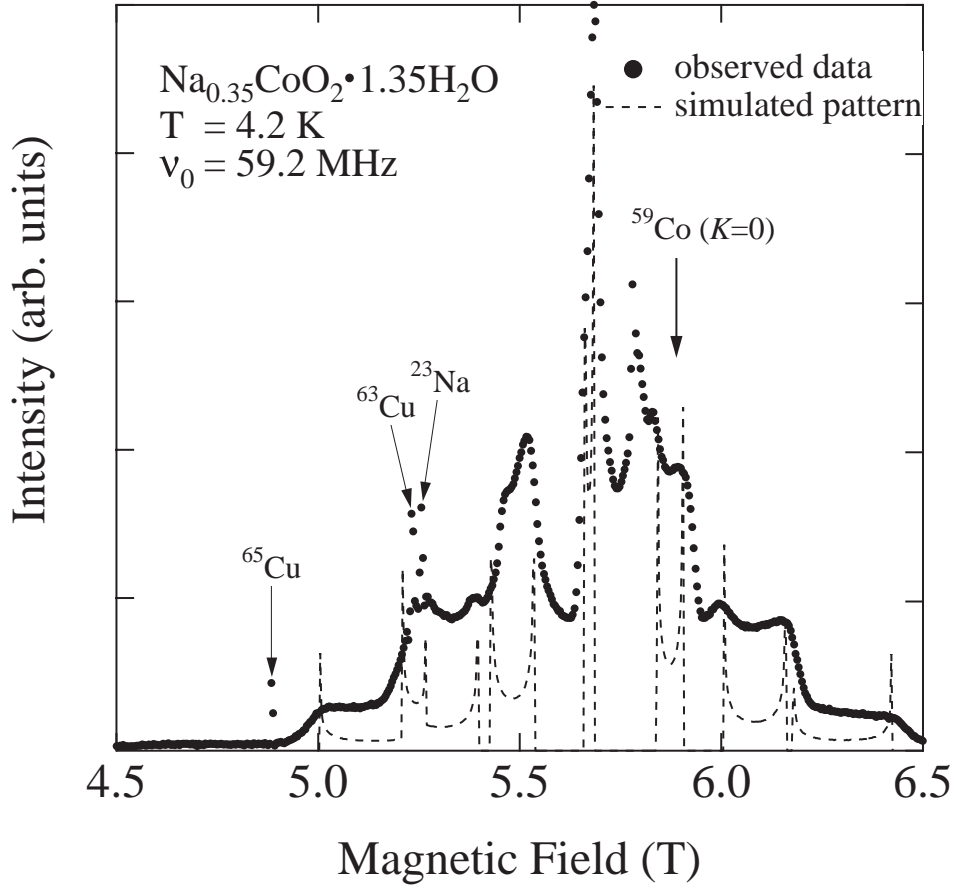


Figure 1. Field-swept NMR spectrum of $\text{Na}_x\text{CoO}_2 \cdot y\text{H}_2\text{O}$ at a constant frequency (ν_0) of 59.2 MHz taken at 4.2 K. Arrows indicate the resonance fields of $^{63,65}\text{Cu}$ nuclei in the resonance coil, ^{23}Na nuclei and the Knight shift reference position ($K = 0$) of ^{59}Co nuclei. Filled circles show the observed data. Dashed line indicates the peak positions and intensities simulated for the case of an anisotropic Knight shift and a second order quadrupole effect with $K_x = 3.56\%$, $K_y = 3.21\%$, $\nu_Q = 4.15$ MHz and the asymmetric parameter of electric field gradient $\eta = 0.21$.

perturbation, a conventional 3D powder pattern of the central transition has five specific resonance frequencies ν_1 - ν_5 in a constant field which are equivalent to resonance fields H_1 - H_5 in a constant frequency (ν_0) [16]. These fields can be observed as two peaks (H_2 and H_4), two shoulders (H_1 and H_5) and a step (H_3) in the case of $\eta < \frac{1}{3}$, where η is the asymmetric parameter of the EFG tensor defined by $\eta = |V_{XX} - V_{YY}|/|V_{ZZ}|$, in which V_{ii} ($ii = XX, YY, ZZ$) are the principal components of the EFG tensor with the relation, $|V_{XX}| \leq |V_{YY}| \leq |V_{ZZ}|$ [16]. In the present case of the 2D powder spectrum, only two peaks appear at specific resonance fields (H_1 and H_2) because of the sample orientation. Hence the central spectrum should consist of two peaks at H_1 and H_2 . Actually, the central resonance was decomposed into two Gaussian components using the least-square fitting to determine the experimental values of H_1 and H_2 as shown in Fig. 2. These resonance fields at a constant frequency ν_0 are expressed by K_j , principal

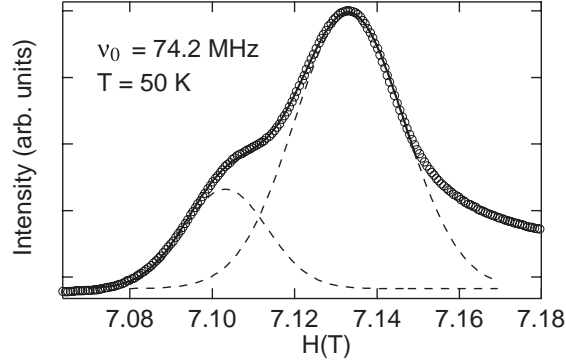


Figure 2. Field-swept NMR spectrum of $\text{Na}_{0.35}\text{CoO}_2 \cdot 1.3\text{H}_2\text{O}$ at $T = 50$ K and $\nu_0 = 74.2$ MHz. Two peaks, which are decomposed by the Gaussian fitting indicated by the dashed lines, correspond to the central resonance of the $I_z = -1/2 \leftrightarrow 1/2$ transition. The anisotropic Knight shifts K_x and K_y were estimated from the low-field smaller peak and the high-field larger peak, respectively (see the text).

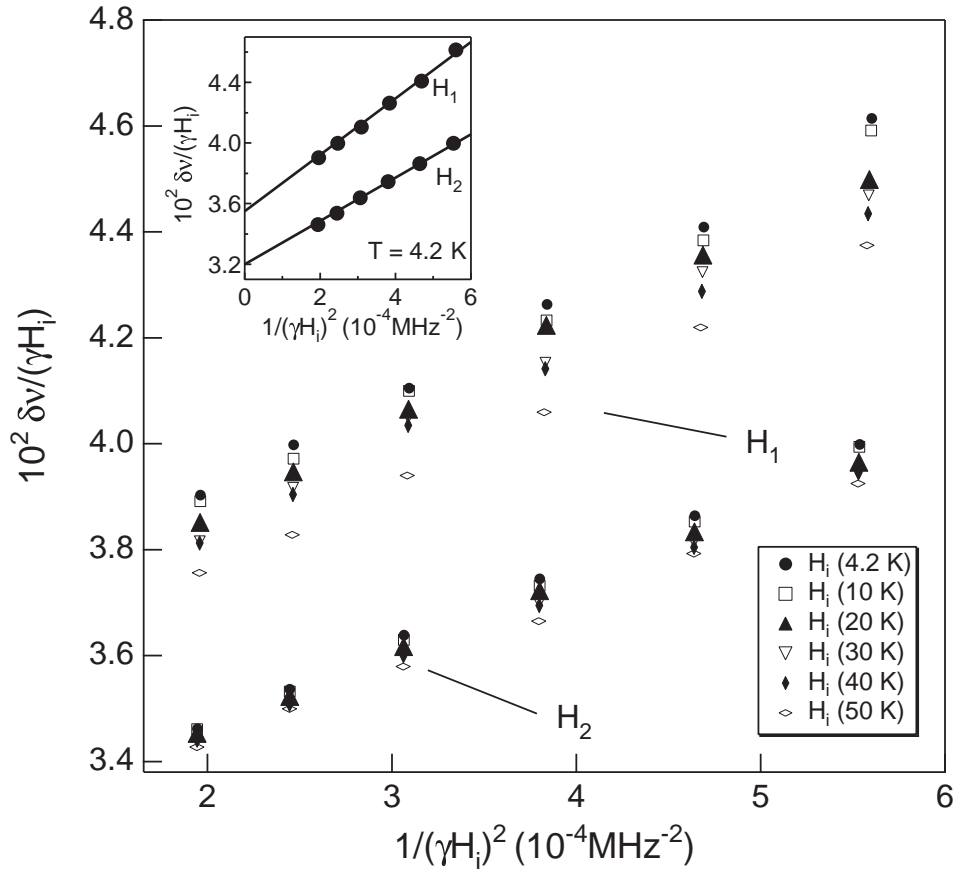


Figure 3. Second-order quadrupole plot at various temperatures above T_c and at 4.2 K (just below T_c) obtained at ν_0 ranging from 44.2 to 74.2 MHz. H_1 and H_2 are the resonance fields at which the ^{59}Co NMR spectrum with 2D powder pattern of the central transition show two singular points. Inset shows the data at 4.2 K with the fitted lines using the NMR parameters, $\nu_Q = 4.15$ MHz, $\eta = 0.21$, $K_x = 3.56$ % and $K_y = 3.21$ %.

values of the Knight shift tensor, and ν_Q , the quadrupole frequency, as follows,

$$\frac{\delta\nu_i}{\gamma_N H_i} = K_j + \frac{C_i}{(1 + K_j)(\gamma_N H_i)^2}, \quad (1)$$

$$\delta\nu = \nu_0 - \gamma_N H_i, \quad (2)$$

$$C_1 = \frac{R(3 + \eta)^2}{144}, C_2 = \frac{R(3 - \eta)^2}{144}, \quad (3)$$

$$R = \nu_Q^2 [I(I + 1) - \frac{3}{4}], \quad (4)$$

where the values with $j = X, Y$ correspond to those with $i = 1, 2$, respectively, γ_N is the nuclear gyromagnetic ratio (10.054 MHz/T for ^{59}Co with the nuclear spin of $I = 7/2$) [16]. As seen in Eq. (1), the linear relation should be expected when $\delta\nu_i/\gamma_N H_i$ is plotted against $(\gamma_N H_i)^{-2}$. Then, the intercepts on the vertical axis at $(\gamma H_i)^{-2} \rightarrow 0$ give the values of K_x and K_y independent of ν_Q .

Figure 3 shows the experimental values of $\delta\nu/(\gamma_N H_i)$ plotted against $(\gamma_N H_i)^{-2}$ ($i = 1, 2$) measured above T_c and at 4.2 K in the frequency range of 44.2 - 74.2 MHz. This plot is referred to a second-order quadrupole plot. The experimental values of $\delta\nu_i/\gamma H_i$ clearly lie on the respective straight lines against $(\gamma H_j)^{-2}$ in the plots. One should note that K_x and K_y (interceptions of the $\delta\nu_i/\gamma_N H_i$ axis) decrease with heating while the slopes are almost independent of T . Since the slope of the line, $C_i/(1 + K_j) (\simeq C_i)$, is determined by ν_Q and η , the almost invariant slope indicates that ν_Q and η are almost constant in this temperature range. This result is consistent with our NQR experiment (not shown here). The inset in Fig. 3 shows the result of the least-square fitting using Eqs. (1)-(4) at 4.2 K. The obtained NMR parameters are $K_x = 3.56\%$, $K_y = 3.21\%$, $\nu_Q = 4.15\text{MHz}$ and $\eta = 0.21$. These parameters at another temperatures were estimated similarly. Using these parameters, we can calculate the simulated spectra as shown by dashed lines in Fig. 1. Consequently, the simulated spectrum including first, second and third satellites is in good agreement with the observed one.

Within the analysis mentioned above, we could not estimate the Z component of the Knight shift due to the 2D sample orientation. However, we have estimated this value as follows. In Fig. 1, we noticed the peak around $H = 5.8$ T, which is not usually expected for the 2D pattern. We regarded this peak as the NMR signals from the accidentally aligned powders along the c -axis. Assuming that this peak corresponds to H_3 , another step in the powder spectrum (a peak in the c -axis oriented spectrum), we have estimated the value of $K_z = 1.88\%$.

In Fig. 4, we indicate the obtained K_x and K_y against the uniform magnetic susceptibility with temperature as an implicit parameter. This is so-called K - χ plot, which is useful for the analysis of various contribution to the Knight shift [17]. For the 3d-transition oxides, the Knight shift can be expressed by

$$K(T) = K_{spin}(T) + K_s + K_{VV}, \quad (5)$$

where $K_{spin}(T)$, K_s and K_{VV} are a T -dependent spin shift, a T -independent spin shift and a Van Vleck orbital shift, respectively. The magnetic susceptibility can be expressed

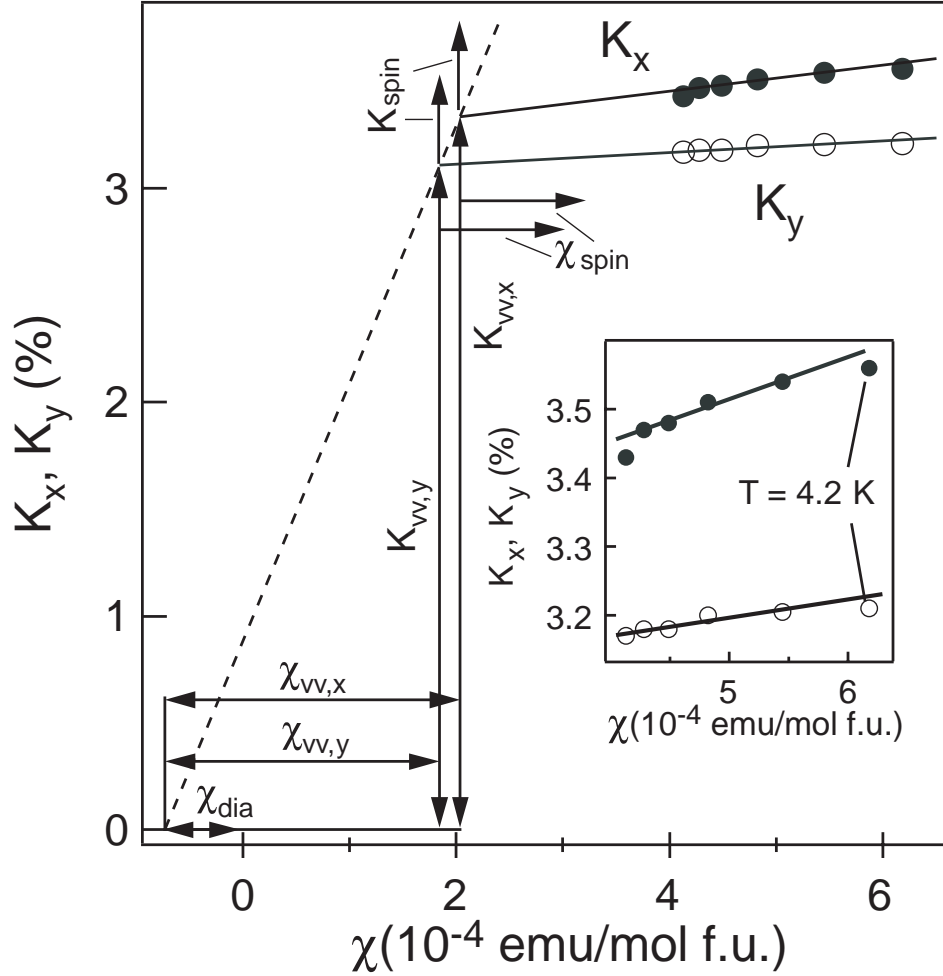


Figure 4. Knight shift vs. susceptibility diagram in $\text{Na}_{0.35}\text{CoO}_2 \cdot 1.3\text{H}_2\text{O}$. The data at 4.2 K (below T_c) is shown for comparison but not used for the line fitting. Inset shows the expansion. The numerical details for constructing the diagram are given in the text. The dashed line is the orbital shift against the orbital susceptibility, $K_{VV} = A_{hf}^{VV} \times \chi_{VV}$.

by,

$$\chi(T) = \chi_{spin}(T) + \chi_s + \chi_{VV} + \chi_{dia}, \quad (6)$$

where $\chi_{spin}(T)$, χ_s , χ_{VV} and χ_{dia} are a T -dependent spin susceptibility, a T -independent spin susceptibility, a Van Vleck orbital susceptibility and a diamagnetic susceptibility at core electrons, respectively. The hyperfine coupling constants connects the respective components of the ^{59}Co Knight shift in Eq. (5) to those of the magnetic susceptibilities in Eq. (6) as follows,

$$K_{spin}(T) = A_{hf}\chi_{spin}(T), \quad (7)$$

$$K_s = A_s\chi_s, \quad (8)$$

$$K_{VV} = A_{VV}\chi_{VV}. \quad (9)$$

The diamagnetic susceptibilities of core electrons can be estimated from relativistic Hartree-Fock calculations. From $\chi_{dia}^{\text{H}} = -0.4 \times 10^{-9} \mu_{\text{B}}/\text{atom}$, $\chi_{dia}^{\text{O}} = -1.6 \times 10^{-9} \mu_{\text{B}}/\text{atom}$, $\chi_{dia}^{\text{Na}} = -3.8 \times 10^{-9} \mu_{\text{B}}/\text{atom}$ and $\chi_{dia}^{\text{Co}} = -5.5 \times 10^{-9} \mu_{\text{B}}/\text{atom}$ [18], the total diamagnetic susceptibility of $\text{Na}_x\text{CoO}_2 \cdot y\text{H}_2\text{O}$ was estimated to be $\chi_{dia} = 7.3 \times 10^{-5} \text{emu/mol}$. The hyperfine coupling constant for the d orbital Van Vleck component, $A_{hf}^{VV} = K_{VV}/\chi_{VV} = 6.7 \times 10^2 \text{ kOe}/\mu_{\text{B}}$ was assumed using $2/\langle r^{-3} \rangle = 9.05 \times 10^{25} \text{ cm}^{-3}$ for Co^{3+} and the reduction factor of 0.8 for the metallic state in compared with the free ion. Using these parameters, the coupling constants for the temperature dependent Knight shift components, A_{hf}^x and A_{hf}^y were estimated to be $+34 \text{ kOe}/\mu_{\text{B}}$ and $+14.7 \text{ kOe}/\mu_{\text{B}}$ by the least-square fitting shown with solid lines in Fig. 4. Then, $\chi_{VV,x}$ and $\chi_{VV,y}$ were estimated to be 2.0×10^{-4} and $1.8 \times 10^{-4} \text{ emu/mol}$ f.u., respectively, and $K_{VV,x}$ and $K_{VV,y}$ to be 3.3 and 3.1 %, respectively, at most. Therefore the spin Knight shifts were found to be $\sim 0.3\%$ for K_x and $\sim 0.1\%$ for K_y at least.

The hyperfine coupling constant A_{hf} between the Co nuclear spin and the electron spins can be expressed by

$$A_{hf} = A_{cp} + A_{dip} + A_{orb} + A_{tr}, \quad (10)$$

where the on-site hyperfine coupling constants of A_{cp} , A_{dip} and A_{orb} are originated from core polarization, dipolar interaction, spin-orbit coupling, respectively, and A_{tr} is from the supertransferred hyperfine field. In $3d$ transition metals, the hyperfine coupling constant due to the core spin polarization of $3d$ electrons is *negative* with $A_{cp} \approx -100 \text{ kOe}/\mu_{\text{B}}$ [19]. The observed *positive* hyperfine coupling constant of $\text{Na}_{0.35}\text{CoO}_2 \cdot 1.3\text{H}_2\text{O}$ is unusual. For some Co-oxides [20, 21, 22] and alloys [23, 24], the *positive* hyperfine coupling constant of ^{59}Co nuclei was observed and attributed to the presence of a large LS-coupling effect. In the present case, a large orbital contribution to K_{spin} via the LS-coupling can account for the *positive* A_{hf} .

In our preliminary experiment for an nonoriented 3D powder sample, K_z is also estimated to be positive $\sim 1.88\%$. Probably the positive coupling constant is caused by not only the anisotropic A_{orb} and A_{dip} but also the transferred hyperfine field A_{tr} . In the present stage, we cannot estimate separately A_{orb} and A_{tr} . The value of K_y is consistent with that reported by Mukhamedshin *et al.*[25].

At first, in the analysis in Fig. 4, we assumed all the temperature independent Knight shift as K_{VV} . However, we must consider the possibility that a part of the spin term does not depend on temperature and K_{VV} is smaller than the estimated value, which should be important when two bands are dominant in the Fermi surface. That is, there must be a finite contribution of K_s in Eq. (5) and χ_s in Eq. (6).

3.2. ^{59}Co Knight shift below T_c

Figure 5 shows the temperature dependence of the central spectra at higher field (about 7 T). Since the estimated upper critical field H_{c2} of $\text{Na}_x\text{CoO}_2 \cdot y\text{H}_2\text{O}$ was reported to be high, 61 T by the magnetization measurement [26] and 17.1 T by the heat capacity

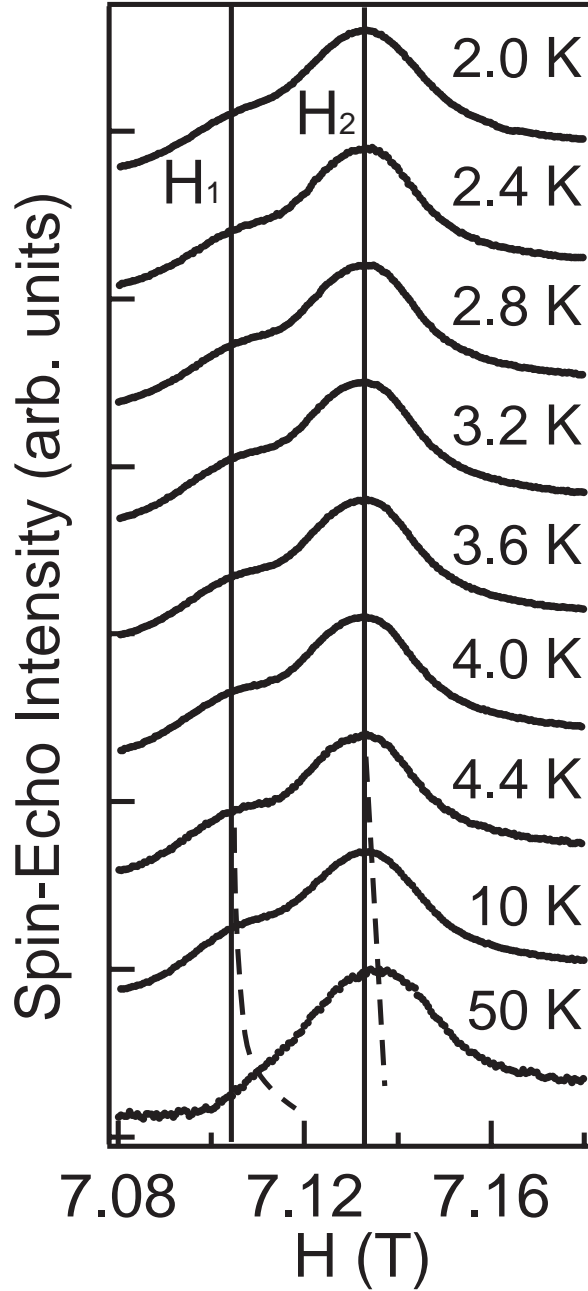


Figure 5. Temperature dependence of the central resonance in the spin echo spectra at ν_0 of 74.2 MHz. Solid lines and dashed curves are guides for eyes. The central resonance field does not change below T_c .

measurement [27], it should be noted that T_c is almost constant, and that samples were in the superconducting state below T_c in our experimental condition. As seen in Fig. 5, the central resonance fields H_1 and H_2 above T_c shift to higher values with increasing temperature, suggesting that the spin contributed Knight shift increases owing to the positive hyperfine coupling constants with a second-order quadrupole shift as discussed above. On the other hand, the values of H_1 and H_2 do not change below T_c , indicating

that K_x and K_y are almost constant at 3.56 and 3.21 % below T_c under the field of about 7 T within an experimental precision. In the BCS theory, the spin susceptibility, χ_{spin} , in the superconducting state is described as

$$\chi_{spin} = -4\mu_B^2 \int_0^\infty N_s(E) \frac{\partial f(E)}{\partial E} dE, \quad (11)$$

where μ_B is Bohr magneton, $N_s(E)$ is the quasiparticle density of states, and $f(E)$ is the Fermi-Dirac distribution function. It is widely known for a singlet pairing superconductor that the spin Knight shift decreases with cooling and vanishes at $T = 0$ in the Yosida function being proportional to $e^{-\Delta(0)/kT}$ at $T \ll T_c$ [28]. The mean free path l is estimated to be $l \geq 100 \text{ \AA}$ from the low-temperature resistivity [29] and the Fermi wave-number k_F [30], and the coherence length ξ to be $\xi \sim 23.2 \text{ \AA}$ [26]. Since the ratio of l/ξ is larger than 4, this system can be considered to be a clean superconductor. Thus, the invariant behavior of K_x and K_y at about 7 T suggests a spin-triplet p - or f -wave pairing superconductivity.

Figure 6 shows the central peaks in the field-swept spectra at 2.0 and 4.2 K at several constant frequencies (44.2 - 74.2 MHz). The resonance fields are almost the same between 2.0 and 4.2 K at $\nu_0 = 74.2 \text{ MHz}$, but it changes drastically at $\nu_0 = 44.2 \text{ MHz}$. The difference of the resonance fields between 2.0 and 4.2 K gradually increases with decreasing the experimental frequency. As well as in the normal state, we discuss the second-order quadrupole plot in the superconducting state shown in Fig. 7. Only H_2 was estimated from the peaks in the spectra, because it was difficult to decompose the spectra especially at lower frequencies. In Fig. 7, the experimental values at 4.4 K show a linear relation similar to those above T_c in Fig. 3. On the other hand, the slope in the superconducting state seems to decrease with temperature, that is, a non-linear relation appears below T_c . Since ν_Q and η are almost constant also below T_c , which were confirmed by our NQR measurements, the decrease of the slope is not due to the change in the quadrupole shift below T_c . Thus, the Knight shift itself must depend on the applied magnetic field.

In Fig. 8, we estimate the temperature dependence of the spin part of the ^{59}Co Knight shift at various resonance frequencies ν_0 below T_c and the Knight shift of ^{23}Na nuclei. This estimation was done by extrapolating from the respective data points in the second-order quadrupole plot in Fig. 7 and Eq. (1), assuming that all the slopes, C_i in Eq. (1), were fixed to be the same value at 4.2 K. As shown in Fig. 8, the temperature-dependent term of the shift increases with decreasing ν_0 . One should note that the values of T_c onsets are almost invariant with changing the magnetic field, which is consistent with the rather high value of H_{c2} . The behavior of the Knight shift below T_c can be explained by a superconducting diamagnetic shift or a field-induced spin Knight shift.

At first we discuss the possibility of the site-dependent diamagnetic effect. The Knight shift of ^{23}Na does not change with $K \sim 0$ indicating that the spin contribution is small and the diamagnetic shift in the superconducting state is also small. The effect of diamagnetic shift was remarkable at the ^{59}Co nuclear sites but negligible at the ^{23}Na

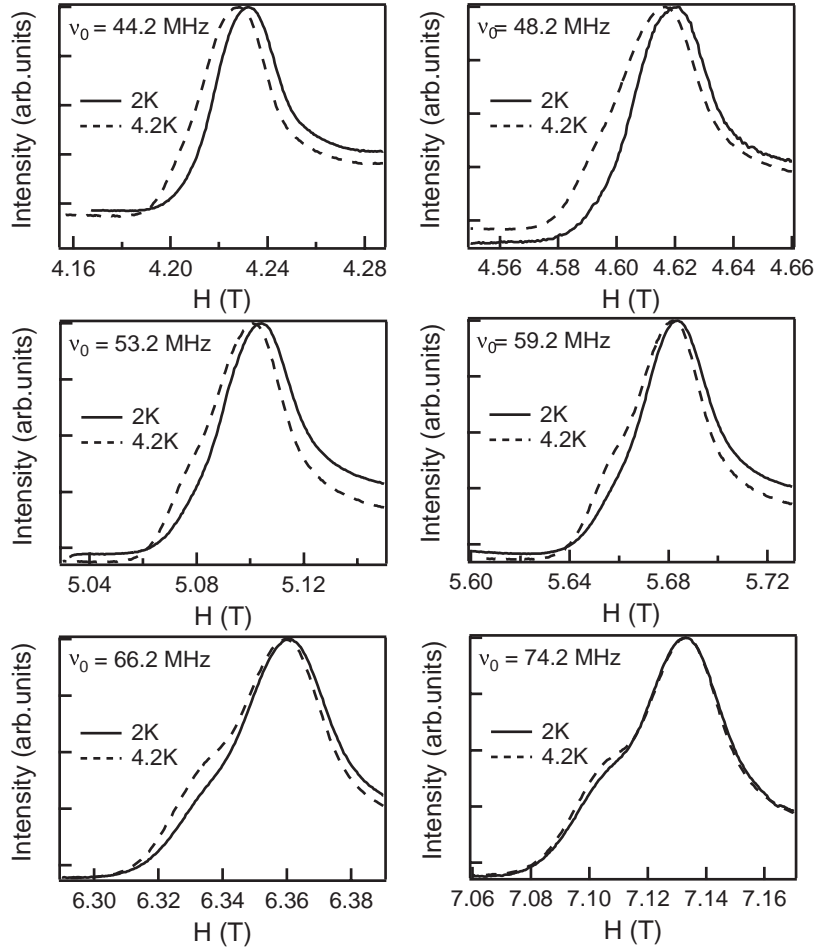


Figure 6. Field-swept 2D powder spectra for the central transition at 2.0 and 4.2 K taken at several fixed frequencies ν_0 .

sites. If Josephson vortices penetrate into the Na layers, the diamagnetic shift due to supercurrents would be expected to be large at the Co sites but not at the Na site. Theoretically, in the vortex state with extremely strong two-dimensional system, that is, with the short coherence length along c -axis, the layer itself works as strong pinning centers of the vortices, resulting in that the diamagnetic effect may depend on the sites in a unit cell [31]. Although in $\text{Na}_{0.35}\text{CoO}_2 \cdot 1.3\text{H}_2\text{O}$, no direct evidence of the intrinsic pinning was obtained, the Josephson vortex can be expected because of the strong two-dimensionality of this compound. Then the invariant behavior of Knight shift at about 7 T should be intrinsic, suggesting the spin triplet superconductivity.

If the change of the resonance fields below T_c at low fields shown in Fig. 6 is not attributed to the diamagnetic effect but due to the change of the intrinsic spin shift, the spin shift decreases with decreasing temperature. In this case, the spin triplet superconductivity with the superconducting d -vector perpendicular to the c -axis as well as the case of the spin singlet superconductivity can be considered. Recent theoretical study suggested that the hole-pocket near the K-point leads the

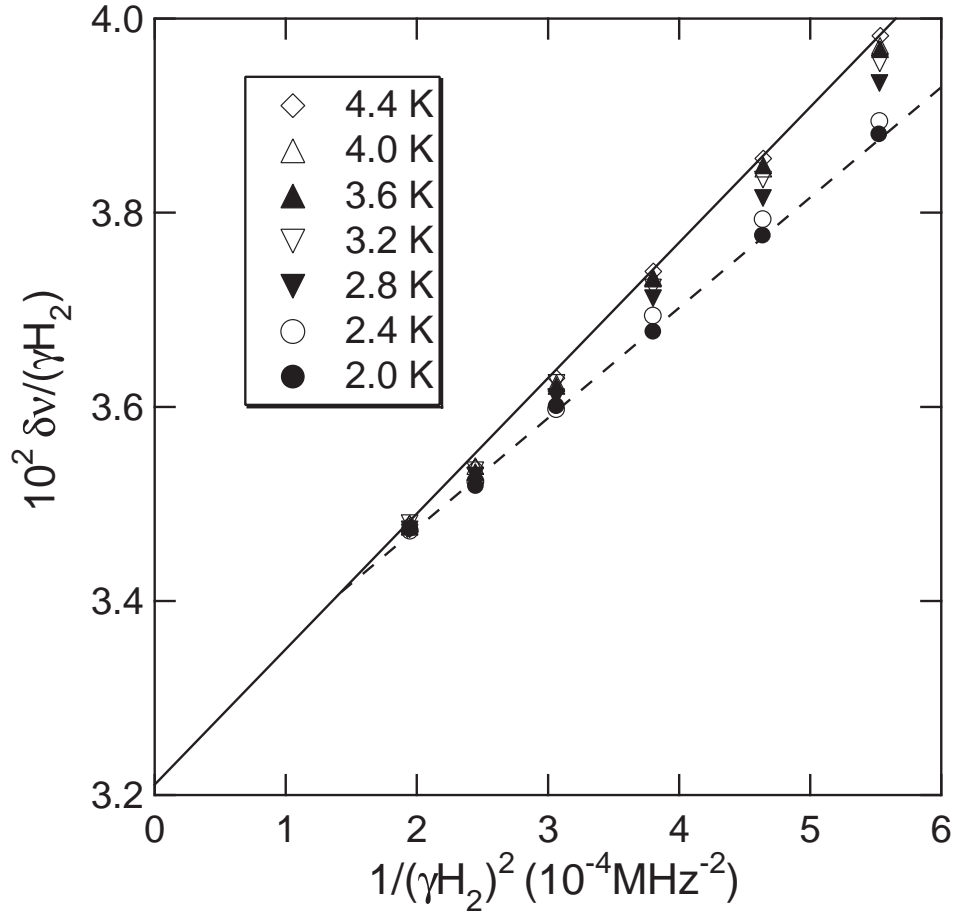


Figure 7. Second-order quadrupole plots for H_2 at various temperatures below T_c . Solid line is the same one for H_2 as shown in the inset of Fig. 3. Dashed line is a guide for eyes. The slope of the linear correlation seems to change below T_c . This is not due to the change of ν_Q nor η but maybe due to the diamagnetic effect.

ferromagnetic fluctuation, resulting in the spin triplet p - or f -wave superconductivity with the d -vector pointing perpendicular to the c -axis in the presence of the strong spin-orbit coupling [32, 33]. A part of the in-plane spin shifts perpendicular to the d -vector may be suppressed at $T = 0$ K. The magnetic field induces the local density of states around the vortex cores, and then a part of the in-plane shift recovers. In this case, the key point is the Knight shift along the c -axis, K_z . In the preliminary results using the resonance center, which is due to the accidental alignment along the c -axis already mentioned, the temperature dependence of K_z above T_c should be very small, suggesting the small contribution of the spin shift, and at least, K_z does not change below T_c .

3.3. ^{59}Co nuclear spin-lattice relaxation time T_1

We measured $1/T_1$ of ^{59}Co under the central resonance field at frequencies of H_2 in order to obtain the information of low lying quasiparticle states below and above

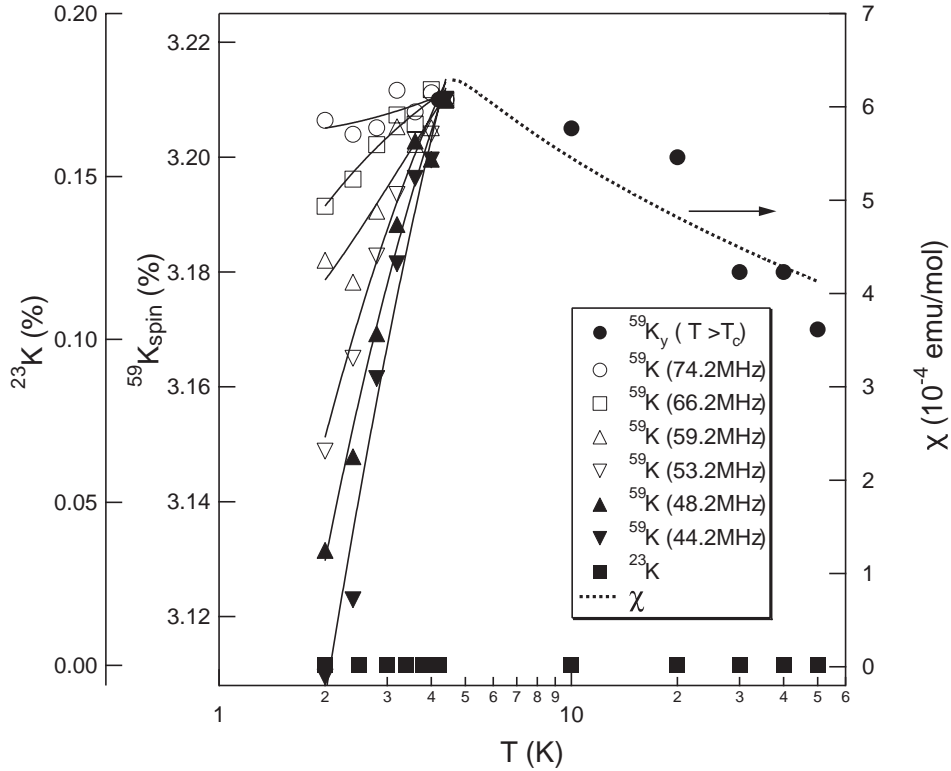


Figure 8. Temperature dependence of the estimated spin part of the Knight shift at various resonance frequencies ν_0 . The data of K_y below T_c were obtained by extrapolation from the respective data points in Fig. 7 and Eq. (1) assuming that ν_Q and η , then C_i in Eq. (1), are the same as those at 4.2 K. Here, a dashed line indicates the temperature dependence of χ . Solid lines are guides for eyes.

T_c . In Fig. 9, we show recovery curves at 4.2 K measured by NQR and NMR (at H_2) methods. The recovery curves for NQR signals at 4.2 K were analyzed by the same function as reported in Refs. [34] and [35]. In the case of NMR, the observed recovery curves were found to consist of more than one relaxation component maybe due to the overlap of satellite resonances in the powder spectrum. Thus, we should utilize the combination of the theoretical relaxation function for the central resonance and a slow single exponential component as follows,

$$\frac{M(\infty) - M(t)}{M(\infty)} = A \left(\frac{1}{84} e^{-\frac{t}{T_1}} + \frac{3}{44} e^{-\frac{6t}{T_1}} + \frac{75}{364} e^{-\frac{15t}{T_1}} + \frac{1225}{1716} e^{-\frac{28t}{T_1}} \right) + B e^{-\frac{t}{T_1^{\text{slow}}}}, \quad (12)$$

where A , B , T_1 and T_1^{slow} are fitting parameters. The solid lines in Fig. 9 are the results of the least-square fitting using Eq. (12). The extrinsic slow component was very small, in which $B/(A+B)$ was found to be about 0.8 %. Figure 10 shows the temperature dependence of $1/T_1 T$ and the inset of the figure shows that of $1/T_1 T$. In NQR measurement, $1/T_1$ rapidly decreases with temperature below T_c with T^3 -dependence. This result is consistent with the data previously reported [34, 35].

Under the field of 7.12 T, the rapid decrease in $1/T_1 T$ is also observed below 4.4 K, which indicates that T_c does not decrease markedly by the external field. We would

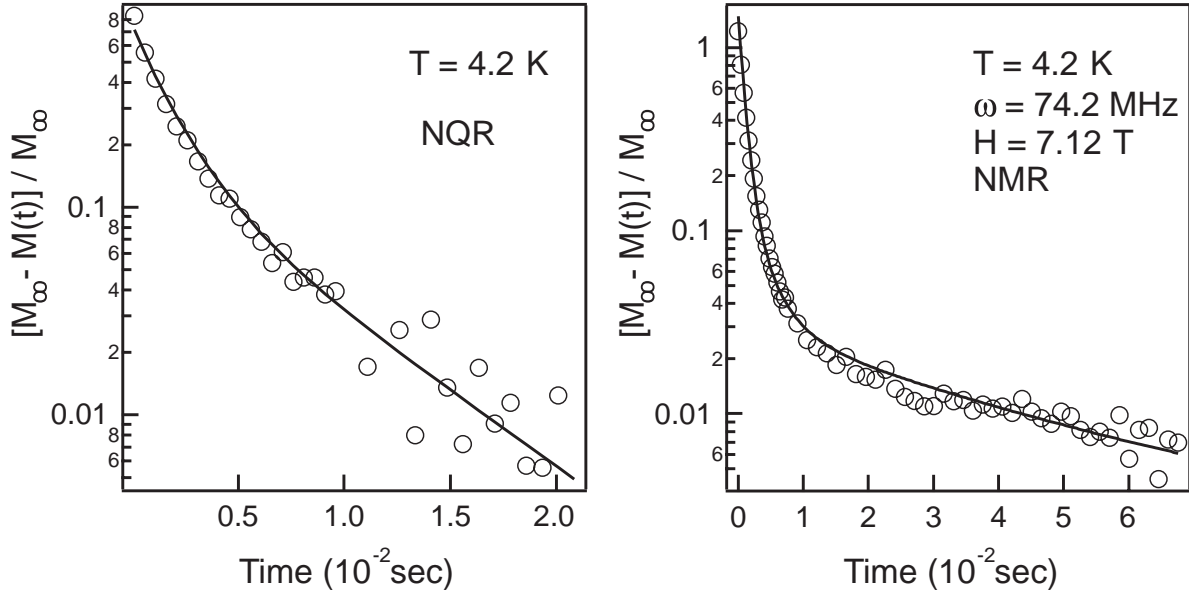


Figure 9. Recovery curves at 4.2 K (a) for the highest frequency transition of ^{59}Co NQR and (b) the center transition of the NMR taken at 74.2 MHz. The values of $1/T_1$ were estimated by the least-square fitting (see the text).

like to note that H_{c2} under the magnetic field parallel to the CoO_2 plane is quite large and T_c decreases very small (estimated about only 0.3 K smaller than that at zero field) at about 7 T. It is also noted that another enhancement of $1/T_1T$ below T_c which may suggest the presence of the unconventional vortex state because this behavior cannot be observed in the NQR measurement under zero magnetic field.

The T^3 dependence of $1/T_1$ below T_c without any coherence peaks indicates the presence of line nodes on the Fermi surface. The recent study on the mother compound Na_xCoO_2 revealed that the ferromagnetic spin fluctuations are dominant in the magnetism on the CoO_2 plane [37]. For our hydrated $\text{Na}_x\text{CoO}_2 \cdot y\text{H}_2\text{O}$, one should note in Fig. 10 that the enhancement of $1/T_1T$ in NQR just above T_c is suppressed at 7.12 T, which indicates that the ferromagnetic fluctuation is dominant in the same temperature range as also suggested by the enhancement of the magnetic susceptibility in Fig. 8. This situation can be suitable for the occurrence of the spin-triplet superconductivity.

4. Summary

From the analysis of the temperature dependence of the field-swept NMR spectra, we estimated the spin component of ^{59}Co Knight shift of $\text{Na}_x\text{CoO}_2 \cdot y\text{H}_2\text{O}$. In the normal state, the in-plane spin Knight shifts were found to be proportional to χ and to have the values of 0.3 and 0.1 % for K_x and K_y at least just above T_c . In the superconducting state, the intrinsic Knight shift does not change with temperature at the external field of about 7 T much smaller than H_{c2} , although the Knight shift is not estimated correctly

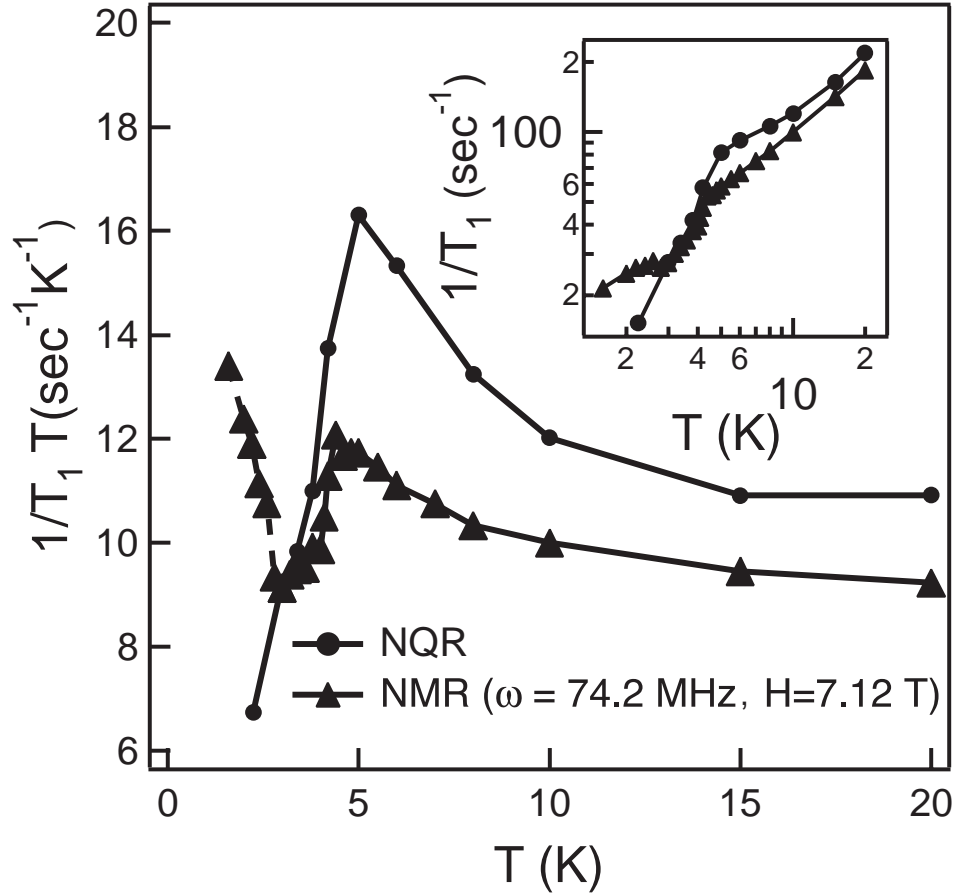


Figure 10. Temperature dependence of $1/T_1T$ for $\text{Na}_x\text{CoO}_2 \cdot y\text{H}_2\text{O}$. Filled circles are by the ^{59}Co NQR data at zero external field and triangles are those of NMR at 7.12 T. The inset shows the temperature dependence of $1/T_1$. One can note that $1/T_1$ decreases proportional to T^3 just below T_c even under $H = 7$ T.

at lower fields because of lack of information of the precise diamagnetic effects. We emphasize that the invariant behavior of the Knight shift in higher fields is consistent with that in μSR experiment [36]. From these results, we conclude that the p - or f - wave pairing state with triplet spin symmetry may be most preferable in the superconducting state of $\text{Na}_x\text{CoO}_2 \cdot y\text{H}_2\text{O}$.

Acknowledgments

This study was supported by a Grant-in-Aid on priority area 'Novel Quantum Phenomena in Transition Metal Oxides', from Ministry of Education, Science, Sports and Culture (12046241, 16076210), and also supported by a Grant-in-Aid Scientific Research of Japan Society for Promotion of Science (14654060, 14740382, 17750059).

References

- [1] K. Takada, H. Sakurai, E. Takayama-Muromachi, F. Izumi, R. A. Dilanian and T. Sasaki, *Nature* **422**, 53 (2003).
- [2] A. Tanaka and X. Hu, *Phys. Rev. Lett.* **91**, 257006 (2003).
- [3] P. W. Anderson, *Mat. Res. Bull.* **8**, 153 (1973).
- [4] G. Baskaran, *Phys. Rev. Lett.* **91**, 097003 (2003).
- [5] B. Kumar and B. S. Shastry, *Phys. Rev. B* **68**, 104508 (2003).
- [6] Q. H. Wang, D. H. Lee and P. A. Lee, *Phys. Rev. B* **69**, 092504 (2004).
- [7] M. Ogata, *J. Phys. Soc. Jpn.* **72**, 1839 (2003)
- [8] K. Kuroki, Y. Tanaka and R. Arita, *Phys. Rev. Lett.* **93**, 077001 (2004).
- [9] R. Arita, K. Kuroki and H. Aoki, *Phys. Rev. B* **60**, 14585 (1999).
- [10] K. Kuroki and R. Arita, *Phys. Rev. B* **63**, 174507 (2001).
- [11] K. Kuroki and R. Arita, *Phys. Rev. B* **64**, 024501 (2001).
- [12] G. Khaliullin, W. Koshibae and S. Maekawa, *Phys. Rev. Lett.* **93**, 176401 (2004).
- [13] Y. Kobayashi, M. Yokoi and M. Sato, *J. Phys. Soc. Jpn.* **72**, 2453 (2003).
- [14] H. Ohta and K. Yoshimura, now in preparation.
- [15] J. F. Baugher, P. C. Taylor, T. Oja and P. J. Bary, *J. Chem. Phys.* **50**, 4914 (1969).
- [16] J. F. Baugher, P. C. Taylor, T. Oja and P. J. Bary, *J. Chem. Phys.* **50**, 4914 (1969).
- [17] J. A. Seitchik, A. C. Gossard and V. Jaccarino, *Phys. Rev.* **4A**, A1119 (1964).
- [18] L. B. Mendelsohn, F. Biggs and J. B. Mann, *Phys. Rev.* **2A**, 1130 (1970).
- [19] A. Freeman and R. E. Watson, "*Hyperfine Interactions in Magnetic Materials*" in *Magnetism* edited by T. Rado and H. Suhl, Academic Press INC..
- [20] M. Itoh and I. Natori, *J. Magn. Magn. Mater.* **140-144**, 2145 (1995).
- [21] K. Miyatani, K. Korn, E. Kamimura and S. Iida, *J. Phys. Soc. Jpn.* **21**, 464 (1966).
- [22] Y. Hayakawa, S. Kohiki, M. Sato, Y. Sonoda, T. Babasaki, H. Deguchi, A. Hidaka, H. Shimooka and S. Takahashi, *Physica E* **9**, 250 (2001).
- [23] A. Narath and D. C. Barham, *Phys. Rev. B* **7**, 2195 (1973).
- [24] R. Dupree, R. E. Walstedt and W. W. Warren, Jr., *Phys. Rev. Lett.* **38**, 614 (1977).
- [25] I. R. Mukhamedshin, H. Alloul, G. Collin and N. Blanchard, *Phys. Rev. Lett.* **94**, 247602 (2005).
- [26] H. Sakurai, K. Takada, S. Yoshii, T. Sasaki, K. Kindo and E. Takayama-Muromachi, *Phys. Rev. B* **68**, 132507 (2003).
- [27] R. Jin, B. C. Sales, S. Li and D. Mandrus, cond-mat/0410517.
- [28] K. Yosida, *Phys. Rev.* **110**, 769 (1958).
- [29] F. C. Chou, J. H. Cho, P. A. Lee, E. T. Abel, K. Matan and Y. S. Lee, *Phys. Rev. Lett.* **92**, 157004 (2004).
- [30] H. -B. Yang, S. -C. Wang, A. K. P. Sekharan, H. Matsui, S. Souma, T. Sato, T. Takahashi, T. Takeuchi, J. C. Campuzano, R. Jin, B. C. Sales, D. Mandrus, Z. Wang and H. Ding, *Phys. Rev. Lett.* **92**, 246403 (2004).
- [31] M. Tachiki and S. Takahashi, *Solid State Commun.* **70**, 291 (1989).
- [32] M. Mochizuki, Y. Yanase and M. Ogata, *J. Phys. Soc. Jpn.* **74**, 1670 (2005).
- [33] Y. Yanase, M. Mochizuki and M. Ogata, private communications.
- [34] T. Fujimoto, G. Zheng, Y. Kitaoka, R. L. Meng, J. Cmaidalka and C. W. Chu, *Phys. Rev. Lett.* **92**, 047004 (2004).
- [35] K. Ishida, Y. Ihara, K. Kitagawa, H. Murakawa, Y. Maeno, C. Michioka, M. Kato, K. Yoshimura, K. Takada, T. Sasaki, H. Sakurai and E. Takayama-Muromachi, *J. Phys. Soc. Jpn.* **72**, 3041 (2003).
- [36] W. Higemoto, K. Ohishi, A. Koda, R. Kadono, K. Ishida, K. Takada, H. Sakurai, E. Takayama-Muromachi and T. Sasaki, *Phys. Rev. B* **70**, 134508 (2004).
- [37] A. T. Boothroyd, R. Coldea, D. A. Tennant, D. Prabhakaran and C. D. Frost, *Phys. Rev. B* **92**, 197201 (2004).